



Evidence for immunomodulation and apoptotic processes induced by cationic polystyrene nanoparticles in the hemocytes of the marine bivalve *Mytilus*



L. Canesi^{a,*}, C. Ciacci^b, E. Bergami^c, M.P. Monopoli^d, K.A. Dawson^d, S. Papa^e,
B. Canonico^b, I. Corsi^c

^a Dept. of Earth, Environmental and Life Sciences-DISTAV, University of Genoa, Italy

^b Dept. of Earth, Life and Environmental Sciences-DISTEVA, University of Urbino, Italy

^c Dept. of Physical, Earth and Environmental Sciences, University of Siena, Italy

^d Centre for BioNanointeractions, School of Chemistry and Chemical Biology, University College Dublin, Ireland

^e Department of Biomolecular Sciences-DISB, University of Urbino, Italy

ARTICLE INFO

Article history:

Received 26 January 2015

Received in revised form

30 April 2015

Accepted 15 June 2015

Available online 16 June 2015

Keywords:

Nanoplastics

Marine invertebrates

Immunity

Apoptosis

ABSTRACT

Polymeric nanoparticles can reach the marine environment from different sources as weathering of plastic debris and nanowaste. Nevertheless, few data are available on their fate and impact on marine biota. Polystyrene nanoparticles (PS NPs) can be considered as a model for studying the effects of nanoplastics in marine organisms: recent data on amino-modified PS NPs (PS-NH₂) toxicity in sea urchin embryos underlined that marine invertebrates can be biological targets of nanoplastics. Cationic PS NPs have been shown to be toxic to mammalian cells, where they can induce apoptotic processes; however, no information is available on their effects and mechanisms of action in the cells of marine organisms. In this work, the effects of 50 nm PS-NH₂ were investigated in the hemocytes of the marine bivalve *Mytilus galloprovincialis*. Hemocytes were exposed to different concentrations (1, 5, 50 µg/ml) of PS-NH₂ suspension in ASW. Clear signs of cytotoxicity were evident only at the highest concentrations (50 µg/ml). On the other hand, a dose dependent decrease in phagocytic activity and increase in lysozyme activity were observed. PS-NH₂ NPs also stimulated increase in extracellular ROS (reactive oxygen species) and NO (nitric oxide) production, with maximal effects at lower concentrations. Moreover, at the highest concentration tested, PS-NH₂ NPs induced apoptotic process, as evaluated by Flow cytometry (Annexin V binding and mitochondrial parameters). The results demonstrate that in marine invertebrates the immune function can represent a significant target for PS-NPs. Moreover, in *Mytilus* hemocytes, PS-NH₂ NPs can act through mechanisms similar to those observed in mammalian cells. Further research is necessary on specific mechanisms of toxicity and cellular uptake of nanoplastics in order to assess their impact on marine biota.

© 2015 Elsevier Ltd. All rights reserved.

1. Introduction

Plastic debris and their degradation products into smaller fragments, at the micro-, and potentially also the nano-scale level, as well as microplastics present in different items, such as cosmetics, are widespread in the marine environment, both in oceans and sediments (Cole et al., 2011; Hidalgo-Ruz et al., 2012; Wright et al.,

2013). Occurrence of nanoplastics in the sea and their possible impact on marine organisms is obviously part of the growing concern for the continuous and increasing release of plastic wastes in the aquatic compartment, including estuarine and coastal areas (Wegner et al., 2012; Corsi et al., 2014). In general, bioavailability of micro- and nano-plastics may depend on their size, density, shape, and surface charges which will affect their behavior in sea water, leading to agglomeration, resuspension and settling; moreover, their uptake, disposal and bioaccumulation by marine organisms is influenced by their feeding behavior, with benthic detritivores and suspension feeders representing more susceptible target species (Wright et al., 2013). Microplastics have been detected in edible

* Corresponding author. DISTAV-Dipartimento di Scienze della Terra, dell'Ambiente e della Vita, Università di Genova, Corso Europa 26, 16132 Genova, Italy.
E-mail address: Laura.Canesi@unige.it (L. Canesi).

marine bivalves, indicating also a possible threat to seafood safety (Van Cauwenberghe and Janssen, 2014).

Polystyrene (PS) is one of the most largely used plastics worldwide, used in food and industrial packaging, disposable cutlery, compact disc cases, building insulation, medical products and toys (Andrady, 2011; PlasticsEurope, 2013). This versatile and non-biodegradable polymer is found in the oceans as micro- and nano-debris, accounting for 24% of the macroplastics in the estuarine habitat (Browne et al., 2008). One of the first evidences of PS impact on filter-feeders is reported by Ward and Kach (2009), showing that marine aggregates of nano-sized PS facilitate food ingestion and are translocated from the gut to the circulatory system, where they are retained for more than a month (Ward and Kach, 2009). Concerning nano-scale PS, only few studies have so far investigated the possible effects in marine species. In the blue mussel *Mytilus edulis*, feeding rate was affected and an increased production of pseudofaeces was observed (Wegner et al., 2012). In our previous study, with sea urchin embryo (*Paracentrotus lividus*), exposure to PS NPs, in particular amino-modified PS NPs (PS-NH₂) caused severe developmental defects (with an EC₅₀ of 3.85 µg/ml) and induced *cas8* gene expression at 24 h post fertilization, suggesting the involvement of apoptotic pathways (Della Torre et al., 2014). However, no information is yet available on the effects of PS NPs at cellular level in marine organisms. The importance of the immune system as a target of NPs toxicity has been already described in two model marine organisms, the bivalve *Mytilus* spp. and the sea urchin *P. lividus* (Canesi et al., 2012; Matranga and Corsi, 2012; Canesi and Procházková, 2013; Corsi et al., 2014). These studies underlined that NPs affect lysosomal function, stimulate the production of reactive oxygen species, and decrease the phagocytic activity in *Mytilus* immune cells, the hemocytes (reviewed in Canesi and Procházková, 2013).

PS NPs are well established in a variety of biological and medical applications including fast synthesis, low costs, easy separation and surface modification. The importance of particle surface functionalization for targeted biomedical application, as well as particle charge as potential determinant factor of cytotoxicity has been underlined in a number of studies on the interactions between functionalized cationic and anionic PS NPs and mammalian cells (Fleischer and Payne, 2014). In particular, cationic particles, such as PS-NH₂, have shown more adverse effects than anionic particles (Liu et al., 2011). A cationic surface would enable the particle to interact with the cell membrane more easily due to their similar molecular structure to proteins, hence, promoting the cell uptake of the NPs (Nel et al., 2009). For example, in human macrophages, PS-NH₂ trigger inflammasome activation and subsequent release of proinflammatory cytokines, induce lysosomal membrane destabilization and release of lysosomal enzymes, as well as production of reactive oxygen species (Lunov et al., 2011). In human astrocytoma cells, PS-NH₂ also induced lysosomal damage and apoptotic processes (Bexiga et al., 2011; Wang et al., 2013). In mammalian cells, different NPs, including PS-NH₂ associate with serum soluble components, organized into a “protein corona”, which affects particle interactions (internalization and effects) (Fleischer and Payne, 2014 and refs. quoted therein). However, no information is available on the interactions of functionalized PS NPs in the cells of marine organisms.

In this work, a battery of functional immune assays was applied to investigate the short term in vitro effects of PS NPs on *Mytilus* immune cells. For this first study, PS-NH₂ were chosen as a model of functionalized PS NPs on the basis of their stronger toxicity demonstrated in both in mammalian cells and the sea urchin. Several functional parameters were evaluated: lysosomal membrane stability and lysosomal enzyme release, extracellular oxyradical production and Nitric Oxide (NO) production, phagocytic

activity, as well as pro-apoptotic processes at both plasma membrane and mitochondrial level.

2. Materials and methods

2.1. Characterization of PS-NH₂ nanoparticles

Primary characterization of unlabeled 50 nm amino polystyrene NPs (PS-NH₂), purchased from Bangs Laboratories, was performed as described in our previous paper (Della Torre et al., 2014). Primary particle diameter of PS-NH₂ was determined by transmission electron microscopy (Philips Morgagni 268D electronics, at 80 KV and equipped with a MegaView II CCD camera. Artificial sea water (ASW) was prepared according to ASTM protocol (pH 8, salinity 36‰) (ASTM, 2004) and filtered with 0.22 µm membrane. PS-NH₂ suspensions (50 µg/ml) were prepared in ASW, quickly vortexed prior to use but not sonicated. Size (Z-average and polydispersity index, PDI) and zeta potential (ζ-potential, mV) were determined by Dynamic Light Scattering (Malvern instruments), using a Zetasizer Nano Series software, version 7.02 (Particular Sciences, UK). Measurements were performed in triplicate, each containing 11 runs of 10 s for determining Z-average, 20 runs for the ζ-potential.

2.2. Animals, hemolymph collection, preparation of hemocyte monolayers and hemocyte treatment

Mussels (*Mytilus galloprovincialis* Lam.) 4–5 cm long, sampled from an unpolluted area at Cattolica (RN) were obtained from SEA (Gabicce Mare, PU) and kept for 1–3 days in static tanks containing artificial sea water (ASW) (1 l/mussel) at 16 °C. Sea water was changed daily. Hemolymph was extracted from the posterior adductor muscle of 8–20 mussels, using a sterile 1 ml syringe with a 18 G1/2" needle. With the needle removed, hemolymph was filtered through a sterile gauze and pooled in 50 ml Falcon tubes at 4 °C. Hemocyte monolayers were prepared as previously described (Canesi et al., 2008). Hemocytes were incubated at 16 °C with different concentrations of PS-NH₂ in ASW, unless otherwise indicated, for different periods of time, depending on the time of endpoint measured. Short-term exposure conditions (from 30 min to 4 h) were chosen to evaluate the rapid in vitro responses to PS-NH₂ at concentrations of 1, 5 and 50 µg/ml (corresponding to 1.46×10^{10} , 7.31×10^{10} , and 7.31×10^{11} particles/ml, respectively), in analogy with those previously observed with other types of NPs in mussel hemocytes (Canesi et al., 2008, 2010; Ciacci et al., 2012) and with studies carried out with functionalized PS NPs in human cells (Lunov et al., 2011; Wang et al., 2013). Untreated (control in ASW) hemocyte samples were run in parallel.

2.3. Hemocyte functional assays

Hemocyte functional parameters (lysosomal membrane stability, lysosomal enzyme release, phagocytosis, extracellular oxyradical production, Nitric oxide production) were evaluated essentially as previously described (Canesi et al., 2008, 2010; Ciacci et al., 2012). Lysosomal membrane stability in control hemocytes and hemocytes pre-incubated with different concentrations of PS-NH₂ (1, 5, 50 µg/ml) for 30 min was evaluated by the Neutral Red Retention time assay. Hemocyte monolayers on glass slides were incubated with 30 µl of an NR solution (final concentration 40 µg/ml from a stock solution of NR 40 mg/ml DMSO); after 15 min excess dye was washed out, 30 µl of ASW, and slides were sealed with a coverslip. Control hemocytes were run in parallel. Every 15 min slides were examined under an optical microscope and the percentage of cells showing loss of the dye from lysosomes in each field was evaluated. For each time point 10 fields were randomly

observed, each containing 8–10 cells. The endpoint of the assay was defined as the time at which 50% of the cells showed sign of lysosomal leaking (the cytosol becoming red and the cells rounded). For each experiment, control hemocyte samples were run in parallel. Triplicate preparations were made for each sample. All incubations were carried out at 16 °C.

Lysosomal enzyme release was evaluated by measuring lysozyme activity in the extracellular medium. To obtain hemolymph serum (i.e., hemolymph free of cells), whole hemolymph was centrifuged at 200× *g* for 10 min, and the supernatant was passed through a 0.22 µm filter. Briefly, lysozyme activity in aliquots of serum of hemocytes incubated with or without PS-NH₂ for different periods of time (from 30 to 60 min) was determined spectrophotometrically at 450 nm utilizing *Micrococcus lysodeikticus*.

Phagocytosis Assay: phagocytosis of neutral red-stained zymosan by hemocyte monolayers was used to assess the phagocytic ability of hemocytes. Neutral red-stained zymosan in 0.05 M Tris–HCl buffer (TBS), pH 7.8, containing 2% NaCl was added to each monolayer at a concentration of about 1:30 hemocytes:zymosan in the presence or absence of PS-NH₂ (1, 5 and 50 µg/ml), and allowed to incubate for 60 min. Monolayers were then washed three times with TBS, fixed with Baker's formal calcium (4%, v/v, formaldehyde, 2% NaCl, 1% calcium acetate) for 30 min and mounted in Kaiser's medium for microscopical examination with a Vanox optical microscope. For each slide, the percentage of phagocytic hemocytes was calculated from a minimum of 200 cells.

Extracellular generation of superoxide was measured by the reduction of cytochrome *c*. Hemolymph was extracted into an equal volume of TBS (0.05 M Tris–HCl buffer, pH 7.6, containing 2% NaCl). Aliquots (500 µl) of hemocyte suspension in triplicate were incubated with 500 µl of cytochrome *c* solution (75 µM ferricytochrome *c* in TBS), with or without PS-NH₂ (final concentration 1, 5, 50 µg/ml). Cytochrome *c* in TBS was used as a blank. Samples were read at 550 nm at different times (from 0 to 30 min) and the results expressed as changes in OD per mg protein.

Nitric oxide (NO) production by mussel hemocytes was evaluated as described previously by the Griess reaction, which quantifies the nitrite (NO₂⁻) content of supernatants. Aliquots of hemocyte suspensions (1.5 ml) were incubated at 16 °C with 1, 5, 10 µg/ml of PS-NH₂ for 0–4 h. Every 60 min, samples were immediately frozen and stored at –80 °C until use. Before analysis, samples were thawed and centrifuged (12,000 × *g* for 30 min at 4 °C), and the supernatants were analyzed for NO₂⁻ content. Aliquots (200 µl) in triplicate were incubated for 10 min in the dark with 200 µl of 1% (wt/v) sulphanilamide in 5% H₃PO₄ and 200 µl of 0.1% (wt/v) N-(1-naphthyl)-ethylenediamine dihydrochloride. Samples were read at 540 nm, and the molar concentration of NO₂⁻ in the sample was calculated from standard curves generated using known concentrations of sodium nitrite.

Finally, the possible effect of hemolymph serum on PS-NH₂-induced lysosomal membrane destabilization were also evaluated. Hemocytes were incubated for 30 min with PS-NH₂ suspensions (1, 5, 50 µg/ml) in filtered hemolymph serum and LMS was evaluated as described above. The results were compared with those obtained in ASW.

2.4. Flow cytometry (FC)

Aliquots of hemolymph were incubated with PS-NH₂ (final concentration 1, 5, 50 µg/ml) for 45 min at 18 °C and analyzed on a FACSCalibur flow cytometer (Becton Dickinson, San Diego, CA, USA). Samples (each containing about 1–2 · 10⁶ cells/mL) were then stained with different fluorescent probes for FC analysis. All incubations were carried out at 18 °C.

Annexin V-FITC and propidium iodide (PI) test was carried out

as previously described (Ciacci et al., 2012): aliquots of 1 ml hemolymph were pelleted by centrifugation (100× *g* for 10 min) and resuspended in 300 µl of annexin-binding buffer (10 mM Hepes and 3.3 mM CaCl₂, pH 7.4) adjusted for salinity by addition of 2% NaCl. FITC-Annexin V (Bender MedSystem, Vienna, Austria) then PI (Sigma) was added to final concentration of 1 mg/ml. Cells were incubated for 15 min in the dark at 16 °C and then processed for FC analyses. For each experimental condition, 10,000 events were collected. Annexin V FITC and PI fluorescence were collected on the logarithmic scale for all experiments.

Mitochondrial parameters were evaluated as previously described (Ciacci et al., 2012). The effects of PS-NH₂ on mitochondrial membrane potential (MMP, Δψ_m) were evaluated by the fluorescent dye Tetramethylrhodamine, ethyl ester perchlorate (TMRE). TMRE is a quantitative marker for the maintenance of the mitochondrial membrane potential and it is accumulated within the mitochondrial matrix in accordance to the Nernst equation. TMRE exclusively stains the mitochondria and is not retained in cells upon collapse of the Δψ_m, which is an early step of apoptotic processes. Hemocytes were incubated with 40 nM TMRE for 10 min before FC analysis using an excitation wavelength of 488 nm and an emission wavelength of 580 nm. Mitochondrial cardiolipin (CL) peroxidation was also evaluated by the CL sensitive probe, 10-nonyl-acridine orange (NAO). After exposure to PS-NH₂, cells were collected by centrifugation, washed in PBS-NaCl buffer, resuspended in the same buffer containing 100 nM NAO and incubated for 30 min. To evaluate changes in fluorescence intensity (FI) values of TMRE and NAO induced by PS-NH₂, we considered the original input on untreated cells as control (100%) (Ciacci et al., 2012).

Sample acquisition and analyses were performed by means of a FACSCalibur flow cytometer equipped with CellQuest™ software and data were expressed as mean ± SD of at least three experiments.

2.5. Confocal microscopy

Cells were exposed to PS-NH₂ (50 and 100 µg/ml) and loaded with TMRE and NAO as described above. Aliquots of samples analysed by flow cytometry were seeded on glass bottom culture dishes; fluorescence of TMRE (excitation 568 nm, emission 590–630 nm), and NAO (excitation 488 nm, emission 490–550 nm) was detected using a Leica TCS SP5 confocal setup mounted on a Leica DMI 6000 CS inverted microscope (Leica Microsystems, Heidelberg, Germany) using 63x 1.4 oil objective (HCX PL APO 63.0 × 1.40 OIL UV). Images were analyzed by the Leica Application Suite Advanced Fluorescence (LASAF) and ImageJ Software (Wayne Rasband, Bethesda, MA).

2.6. Statistics

Data are the mean ± SD of at least 3 independent experiments in triplicate. Statistical analysis was performed by using ANOVA plus Tukey's post hoc test.

3. Results

3.1. Particle characterization

In Fig. 1 and Table 1 are reported data on characterization of primary PS-NH₂ particles and of particle suspension in ASW. TEM analysis (Fig. 1A) of PS-NH₂ confirmed their nominal size of 50 nm reported by Della Torre et al. (2014). DLS analysis of PS-NH₂ suspensions in ASW (50 µg/ml) revealed the formation of small aggregates with a Z-average of 200.3 nm, a PDI of 0.302 and a ζ-

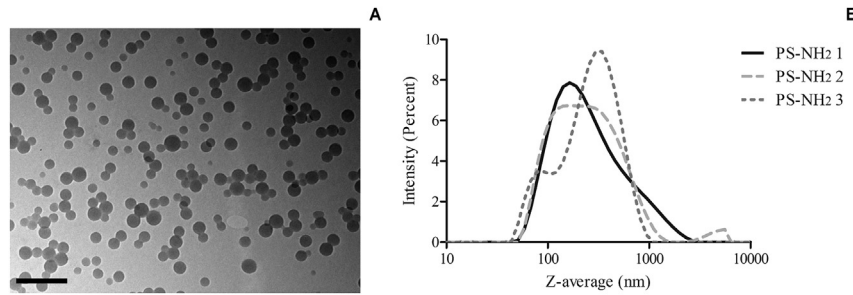


Fig. 1. Primary and secondary characterization of PS-NH₂ using TEM imaging and DLS, respectively. Left: TEM image of primary 50 nm PS-NH₂. Scale bar: 200 nm. Right: Size distribution graph by intensity for PS-NH₂ suspension at 50 µg/ml in ASW, determined by Contin analysis (DLS Analysis). Three independent replicates are shown, the x-axis minimum set at 10 nm and a logarithmic scale is used for y-axis. The graph was edited using GraphPad Prism5.

Table 1

Physico-chemical characterization of PS-NH₂ in Milli-Q water and artificial sea water (ASW) (0.22 µm filtered, T = 18 °C, salinity 36‰, pH 8) using DLS analysis showing Z-average (nm), polydispersity index (PDI) and ζ-potential (mV). Data are referred to PS-NH₂ concentration of 50 µg/ml and values reported as mean ± standard deviation.

| | 50 nm PS-NH ₂ | | |
|--------|--------------------------|--------------|------------------|
| | Z-Average (nm) | PDI | ζ-potential (mV) |
| MilliQ | 57 ± 2 | 0.07 ± 0.02 | +43 ± 1 |
| ASW | 200 ± 6 | 0.302 ± 0.02 | +14 ± 2 |

potential of +14.2 mV (Fig. 1B and Table 1). Behavior of PS-NH₂ in ASW was similar to that previously observed in natural sea water (NSW) (Della Torre et al., 2014); in contrast, when particles were suspended in MilliQ water, no agglomeration occurred and a higher ζ-potential was observed (+43 ± 1 mV) (Table 1). Lower absolute values of ζ potential observed in both ASW and NSW (as compared to those measured in MilliQ water, suggest a screening effect of surface charges due to the higher salt content.

3.2. Effects of PS-NH₂ on hemocyte functional parameters

The effects of PS-NH₂ on *Mytilus* hemocytes were evaluated using a battery of assays, utilizing different exposure times (from 30 min to 4 h) and conditions optimized for each assay as previously described (Ciacci et al., 2012). Lysosomal membrane stability (LMS) and lysozyme release were evaluated in hemocytes incubated with different concentrations of PS-NH₂ (1, 5 and 50 µg/ml) and the results are reported in Fig. 2. As shown in Fig. 2A, a dose dependent decrease in LMS was observed (−50% at the highest

concentration tested; $p < 0.05$). Incubation with PS-NH₂ for different periods of time induced significant lysozyme release (Fig. 2B). Interestingly, both 5 and 50 µg/ml induced a large lysozyme release immediately after addition (up to +150% with respect to controls with the highest concentration; $p < 0.05$), whereas after 30 min incubation a comparable increase was observed at all the concentrations tested (about +100%; $p < 0.05$). On the other hand, no effect was observed at longer incubation times.

PS-NH₂ stimulated total extracellular oxyradical (or reactive oxygen species-ROS) production, evaluated as cytochrome c reduction at all the concentrations tested, with the highest increase observed at the lowest concentration (about three-folds with respect to controls, $p < 0.05$) (Fig. 3A). Nitric oxide-NO production was evaluated as nitrite accumulation in hemocytes incubated with PS-NH₂ for different periods of time (from 1 to 4 h) (Fig. 3B). Significant increases were observed at different concentrations, with the highest concentration stimulating NO production at all times of exposure. However, the strongest effects were observed at 2 h incubation, with 5 µg/ml eliciting the highest response. Finally, PS-NH₂ induced a dose dependent decrease in phagocytosis, that was significant from 1 µg/ml and maximal at 50 µg/ml (−16 and −50%, respectively; $p < 0.05$) (Fig. 4).

3.3. Effects on apoptotic parameters

The effects of PS-NH₂ incubation (45 min) on apoptotic parameters at both plasma membrane and mitochondrial level were evaluated by Flow Cytometry utilizing specific fluorescent dyes for phosphatidylserine externalization (Annexin V binding), mitochondrial membrane potential Δψ_m (Tetramethylrhodamine, ethyl ester perchlorate-TMRE) and cardiolipin peroxidation in the inner

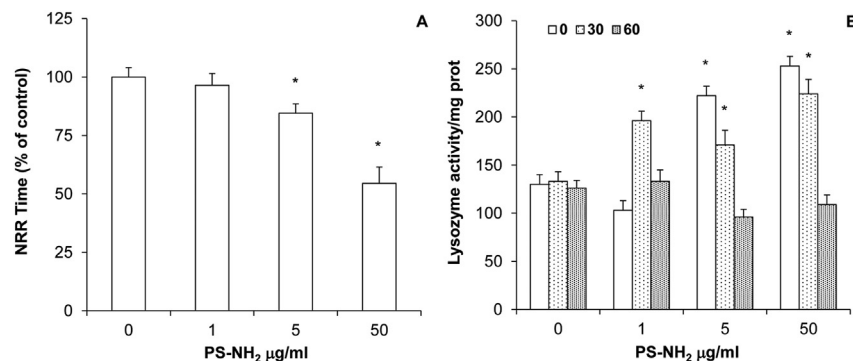


Fig. 2. Effects of PS-NH₂ (1, 5, 50 µg/ml) on mussel hemocytes: A) Lysosomal membrane stability-LMS; B) extracellular lysozyme release, evaluated at different times of incubation (30 and 60 min). Data, representing the mean ± SD of four experiments in triplicate, were analysed by ANOVA followed by Tukey's post hoc test. Significant differences with respect to controls ($p \leq 0.05$) are reported (*).

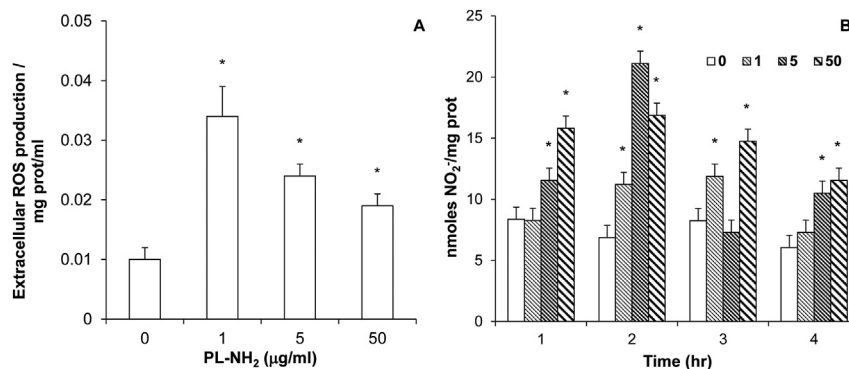


Fig. 3. Effects PS-NH₂ (1, 5, 50 µg/ml) on oxyradical and NO production by mussel hemocytes. A) extracellular oxyradical production, evaluated as cytochrome c reduction in control hemocytes and hemocytes exposed to PS-NH₂ for 30 min; B) NO production, evaluated as nitrite accumulation by the Griess reaction, evaluated in control and PS-NH₂-exposed hemocytes at different times of incubation (from 1 to 4 h). Data, representing the mean \pm SD of four experiments in triplicate, were analysed by ANOVA followed by Tukey's post hoc test. Significant differences with respect to controls ($p < 0.05$) are reported (*).

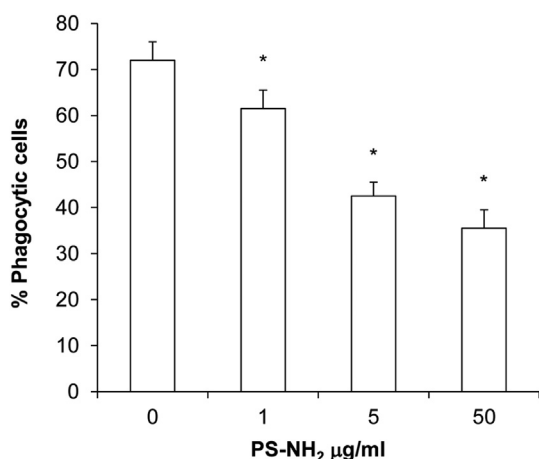


Fig. 4. Effects PS-NH₂ (1, 5, 50 µg/ml) on phagocytic activity of mussel hemocytes, evaluated as uptake of Neutral-Red conjugated zymosan particles. Data, expressed as percentage of phagocytic cells and representing the mean \pm SD of four experiments in triplicate, were analysed by ANOVA followed by Tukey's post hoc test. Significant differences with respect to controls ($p < 0.05$) are reported (*).

mitochondrial membrane (10-nonyl-acridine orange-NAO), and the results are reported in Fig. 5. A significant increase in Annexin V positive-hemocytes was induced by the highest concentration tested (+30% with respect to control; $p < 0.05$) (Fig. 5A). A small but significant increase in the percentage of Annexin V/PI positive cells, indicating necrotic processes, was also observed. At 50 µg/ml, significant decreases in TMRE fluorescence indicated decreases in mitochondrial membrane potential $\Delta\psi_m$ (−23% with respect to control; $p < 0.05$); moreover, decreased NAO fluorescence indicated cardiolipin peroxidation in the inner mitochondrial membrane (−20%; $p < 0.05$). Such decreases in fluorescence could not be easily appreciated by microscopical observations; however, when cells were exposed to higher PS-NH₂ concentrations (100 µg/ml), larger decreases in both TMRE and NAO fluorescence were observed, as shown by representative images obtained by confocal microscopy (Fig. 5B).

3.4. Effects of hemolymph serum on PS-NH₂-induced lysosomal damage

Hemocyte LMS was also evaluated in samples incubated for 30 min with PS-NH₂ in the presence hemolymph serum (1, 5, 50 µg/ml), and the results were compared with those obtained in ASW. As

shown in Fig. 6, a clear dose-dependent decrease in LMS was clearly observed (−32, −51 and −66% respectively; $p < 0.05$). Such an effect was stronger than that observed in ASW at all the concentrations tested, indicating that the hemolymph soluble fraction significantly increased lysosomal damage induced by PS-NH₂.

4. Discussion

In mammalian cells, the adverse effects of NPs, including nanoplastics, are commonly observed through measuring different physiological endpoints, including those related to lysosomal function, oxidative stress, inflammation, apoptosis (Bexiga et al., 2011; Lunov et al., 2011; Stern et al., 2012; Wang et al., 2013; Fleischer and Payne, 2014). In this work, a battery of functional assays was applied to investigate the possible effects of PS-NH₂ in the immune cells, the hemocytes, of the marine bivalve *M. galloprovincialis*.

With regards to characterization of PS-NH₂ suspensions, the low aggregation shown by PS-NH₂ in ASW (Fig. 1) is still slightly higher compared to what observed in natural sea water and reported in our previous study (Della Torre et al., 2014). Further, the measured ζ -potential as +14.2 mV resulted lower than that obtained in MilliQ water (+42.8 mV) (data not shown), indicating a screening effect of surface charges due to the higher salt content of ASW.

The results show that short term exposure (30 min) to PS-NH₂ induced rapid lysosomal destabilization at increasing concentrations. PS-NH₂ were able to stimulate lysosomal enzyme release, evaluated as extracellular lysozyme activity, also at concentrations as low as 1 µg/ml, with maximal effects at 30 min at all the concentrations tested. PS-NH₂ also induced extracellular oxyradical production, as well as NO production, with significant effects at lower concentrations (1–5 µg/ml). Finally, a dose dependent decrease in phagocytic activity was also observed. Overall, the results indicate that lower concentrations of PS-NH₂ elicited the release of hydrolytic enzymes and oxygen and nitrogen based reactive species, which represents the first inflammatory response induced by non-self material. On the other hand, at higher concentrations (50 µg/ml), a dramatic decrease in phagocytosis and strong lysosomal destabilization were observed, indicating impairment of immunocompetence and lysosomal damage. These data were supported by the results obtained on apoptotic parameters evaluated by flow cytometry. At 50 µg/ml PS-NH₂ induced significant increases in Annexin V staining, indicating phosphatidylserine externalization at the plasma membrane, as well as decreases in mitochondrial membrane potential and increased cardiolipin peroxidation in the inner mitochondrial membrane; all

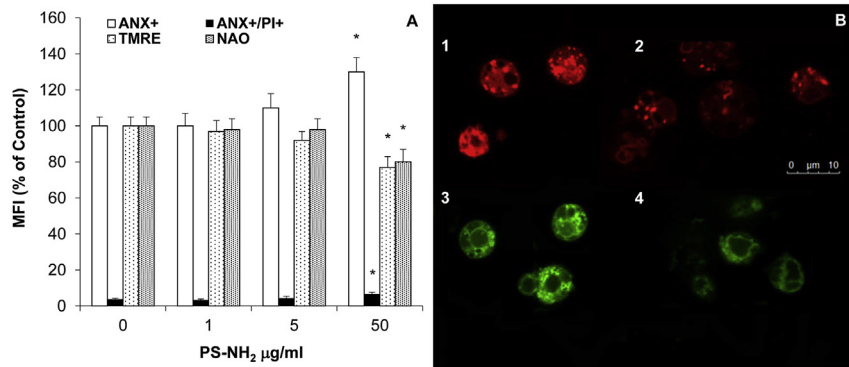


Fig. 5. Effect of PS-NH₂ on apoptotic parameters of mussel hemocytes. A) Flow cytometry: hemocytes were exposed to PS-NH₂ (1, 5, 50 µg/ml) for 45 min, subsequently loaded with different fluorescent dyes and analysed as described in Methods. Percentage of hemocytes positive to FITC Annexin V binding (ANX+) and to both ANX and PI staining (ANX+/PI+) are reported. For mitochondrial parameters, cells were loaded with TMRE (for membrane potential $\Delta\psi_m$) and with NAO for cardiolipin content. Data are reported as Mean Fluorescence Intensities (MFI) (% with respect to controls). Data, representing the mean \pm SD of three experiments, were analysed by ANOVA followed by Tukey's post hoc test. Significant differences with respect to controls ($p < 0.05$) are reported (*). B) Confocal fluorescence microscopy: representative confocal images of hemocytes exposed in the same experimental conditions to PS-NH₂ (100 µg/ml) and loaded with TMRE or NAO for determination of mitochondrial parameters. 1–2: TMRE (543 excitation/633 emission filter set, red); 3–4: NAO (518 excitation/530 emission filter set, green) (60 \times magnification). 1: Control TMRE; 2: PS-NH₂ TMRE; 3: Control NAO; 4: PS-NH₂ NAO. A decrease in both TMRE and NAO fluorescence can be appreciated in cells exposed to PS-NH₂ compared to untreated cells. (For interpretation of the references to color in this figure legend, the reader is referred to the web version of this article.)

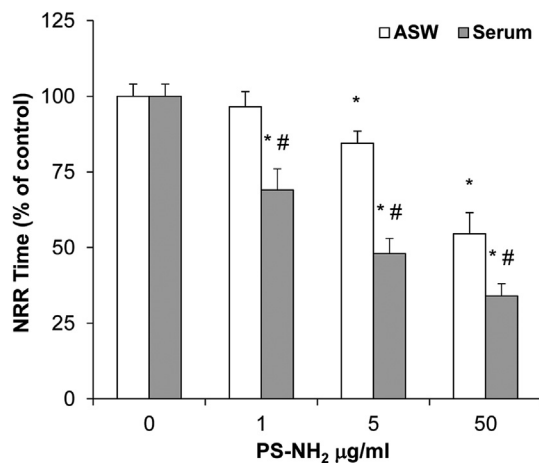


Fig. 6. Effects of hemolymph serum on PS-NH₂ – induced lysosomal membrane destabilization in mussel hemocytes. Cells were incubated as described in methods with PS-NH₂ suspensions (1, 5, 50 µg/ml) in either ASW or in hemolymph serum. Data, representing the mean \pm SD of four experiments in triplicate, were analysed by ANOVA followed by Tukey's post hoc test ($p \leq 0.05$). * = all treatments vs controls; # = serum vs ASW.

these effects were detected as early as 45 min of exposure. Interestingly, further increasing PS-NH₂ concentration (up 100 µg/ml) resulted in larger decreases in both TMRE and NAO fluorescence (about 60% and 40%, respectively; not shown) that could be easily appreciated by confocal microscopy. Pre-apoptotic signs at mitochondrial level were previously observed in hemocytes exposed to nanosized carbon black (NCB) (Canesi et al., 2008) and ZnO NPs (Ciacci et al., 2012). In contrast, in human cells, PS-NH₂ induced lysosomal damage at longer times of incubation (within 3–6 h of exposure), whereas phosphatidylserine exposure and loss of mitochondrial membrane potential could be detected after 6–8 h exposure (Wang et al., 2013). From these data obtained in human cells, a description of the evolution of apoptotic cell death in which lysosomal damage plays a central role has been hypothesized for PS-NH₂ (Wang et al., 2013). This could also apply to the cells of marine invertebrates; actually, the first indication of interactions of NPs with bivalve cells was the observation of endosomal and lysosomal accumulation and oxyradical production following

endocytosis of Nile red labeled sucrose polyester nanoparticles in isolated *Mytilus* digestive gland cells (Moore, 2006). Induction of apoptotic pathways has been also observed in the sea urchin embryo exposed to PS-NH₂ at 24 h post fertilization (Della Torre et al., 2014). Moreover, our results, indicating common mechanisms of action of PS-NH₂ in *Mytilus* hemocytes and human cells, suggest that similar pathways may be activated in the cells of marine invertebrates. In mussel hemocytes, functional responses as well as cellular damage and induction of apoptotic processes were particularly rapid, occurring within 1 h of exposure. This is in line with the physiological role of hemocytes, which are responsible for cell mediated immunity and represent the first line of defence against non self material in bivalves (Canesi et al., 2002; Canesi and Procházková, 2013).

The evaluation of the biological effects of NPs requires a molecular-level understanding of how NPs interact with cells in a physiological environment. In mammalian systems, extracellular serum proteins adsorb onto the NP surface, forming a protein “corona” (Lundqvist et al., 2008; Fleischer and Payne, 2014 and refs. quoted therein). The protein corona formed by both PS-NH₂ and PS-COOH has been recently investigated in detail, underlying the role of albumin (BSA), the major serum protein (Fleischer and Payne, 2014). The results obtained in this work showed that the presence of hemolymph serum significantly increased the lysosomal damage induced by PS-NH₂ in the hemocytes, with significant effects at concentrations as low as 1 µg/ml. These data, although preliminary, underline how also in *Mytilus* soluble serum components can affect NP interactions with cells, and suggest that an NP-protein corona might also be formed in biological fluids of marine invertebrates. This possibility is intriguing, since the corona proteins control the specific cellular receptors used by protein-NP complex, the cellular internalization pathways, and the immune response (Fleischer and Payne, 2014 and refs. quoted therein). Soluble hemolymph components of *Mytilus* hemolymph have been recently characterized (Oliveri et al., 2014), demonstrating that the Extrapallial Protein (EP) precursor, or putative C1q domain containing protein MgC1q6, represents the most abundant serum protein in mussels. Since understanding the protein corona is crucial for understanding how NPs interact with cells *in vivo*, interactions of NPs, including PS-NH₂, with hemolymph serum proteins deserve further investigation.

Acute ecotoxicity of cationic PS-NPs was assessed on a test battery of freshwater organisms representing different trophic levels (Casado et al., 2013). However, toxic effects were observed at high concentration, where high agglomeration and sedimentation of NPs were observed, this underlying the unsuitability of classical ecotoxicity tests for NP assessment. Apart from traditional ecotoxicity testing, it has been underlined how more specific assays, like immunotoxicity tests, may help understanding the major toxic mechanisms and modes of action that could be relevant for different nanomaterials in different organisms (Crane et al., 2008). Cell-mediated immunity and the phagocytic cells are being identified as the primary target of NPs in aquatic organisms (Jovanovic and Palic, 2012). The results obtained in mussel hemocytes represent the first data on the effects and mechanisms of action of nanoplastics at a cellular level in marine organisms. Overall, the results demonstrate that in *Mytilus* hemocytes PS-NH₂ elicited rapid effects also at low concentrations, with mechanisms similar to those observed in mammalian cells. The application of a battery of functional tests on *Mytilus* hemocytes has been proven as a powerful tool for the rapid screening of the immunomodulatory effects of different types of NPs in cell models of marine organisms, as well as robust alternative methods for testing the toxicity of NPs and a possible basis for designing of environmentally safer nanomaterials (reviewed in Canesi et al., 2012; Canesi and Procházková, 2013). This may also apply to nanoplastics and may help understanding their possible impact in the marine environment.

Despite many studies have described the increasing occurrence of microplastic in the marine environment (Andrady, 2011; Cole et al., 2011; Hidalgo-Ruz et al., 2012; Wright et al., 2013), much less is known about their degradation into smaller particles and no data on nanoplastic concentrations in environmental samples are available yet. However, nanoplastics may become a threat in the future for marine organisms when the large amount of microplastic decays, and with the rapidly increasing industrial production of NPs, including nanoplastics, for all kinds of applications (Wegner et al., 2012), with predicted concentrations for most nanomaterials higher than in 2009 (Sun et al., 2014). Moreover, sorption of other chemical pollutants to nanoplastics, like to other NPs, may affect their biological impact (Canesi et al., 2015). In this light, further studies are needed to investigate the potential effects of nanoplastics on marine organisms.

Acknowledgments

PS NPs secondary characterisation was performed by Second Level degree student Elisa Bergami at the Centre for BioNano Interactions (University College of Dublin) funded by the Erasmus Long Life Learning Programme (year 2012–2013).

References

- Andrady, A.L., 2011. Microplastics in the marine environment. *Mar. Pollut. Bull.* 62, 1596–1605.
- ASTM, 2004. International Standard Guide for Conducting Static Acute Toxicity Tests Starting with Embryos of Four Species of Salt Water Bivalve Mollusks, pp. E 724–798.
- Bexiga, M.G., Varela, J.A., Wang, F., Fenaroli, F., Salvati, A., Lynch, I., Simpson, J.C., Dawson, K.A., 2011. Cationic nanoparticles induce caspase 3-, 7- and 9-mediated cytotoxicity in a human astrocytoma cell line. *Nanotoxicology* 5, 557–567.
- Browne, M.A., Dissanayake, A., Galloway, T.S., Lowe, D.M., Thompson, R.C., 2008. Ingested microscopic plastic translocates to the circulatory system of the mussel, *Mytilus edulis* (L.). *Environ. Sci. Technol.* 42, 5026–5031.
- Canesi, L., Procházková, P., 2013. The invertebrate immune system as a model for investigating the environmental impact of nanoparticles. In: Boraschi, D., Duschl, A. (Eds.), *Nanoparticles and the Immune System*. Acad. Press, Oxford, pp. 91–112.
- Canesi, L., Gavioli, M., Pruzzo, C., Gallo, G., 2002. Bacteria – hemocyte interactions and phagocytosis in marine bivalves. *Microsc. Res. Tech.* 57, 469–476.
- Canesi, L., Ciacci, C., Betti, M., Fabbri, R., Canonico, B., Fantinati, A., Marcomini, A., Pojana, G., 2008. Immunotoxicity of carbon black nanoparticles to blue mussel hemocytes. *Environ. Int.* 34, 1114–1119.
- Canesi, L., Ciacci, C., Vallotto, D., Gallo, G., Marcomini, A., Pojana, G., 2010. In vitro effects of suspensions of selected nanoparticles (C60 fullerene, TiO₂, SiO₂) on *Mytilus* hemocytes. *Aquat. Toxicol.* 96, 151–158.
- Canesi, L., Ciacci, C., Fabbri, R., Marcomini, A., Pojana, G., Gallo, G., 2012. Bivalve molluscs as a unique target group for nanoparticle toxicity. *Mar. Environ. Res.* 76, 16–21.
- Canesi, L., Ciacci, C., Balbi, T., 2015. Interactive effects of nanoparticles with other contaminants in aquatic organisms: friend or foe? *Mar. Environ. Res.* <http://dx.doi.org/10.1016/j.marenvres.2015.03.010>.
- Casado, M.P., Macken, A., Byrne, H.J., 2013. Ecotoxicological assessment of silica and polystyrene nanoparticles assessed by a multitrophic test battery. *Environ. Int.* 51, 97–105.
- Ciacci, C., Canonico, B., Bilaničová, D., Fabbri, R., Cortese, K., Gallo, G., Marcomini, A., Pojana, G., Canesi, L., 2012. Immunomodulation by different types of n-oxides in the hemocytes of the marine bivalve *Mytilus galloprovincialis*. *PLoS One* 7, e36937.
- Cole, M., Lindeque, P., Halsband, C., Galloway, T.S., 2011. Microplastics as contaminants in the marine environment: a review. *Mar. Pollut. Bull.* 62, 2588–2597.
- Corsi, I., Cherr, G.N., Lenihan, H.S., Labille, J., Hasselov, M., Canesi, L., Dondero, F., Frenzilli, G., Hristozov, D., Puentes, V., Della Torre, C., Pinsino, A., Libralato, G., Marcomini, A., Sabbioni, E., Matranga, V., 2014. Common strategies and technologies for the ecosafety assessment and design of nanomaterials entering the marine environment. *ACS Nano* 8, 9694–9709.
- Crane, M., Handy, R.D., Garrod, J., Owen, R., 2008. Ecotoxicity test methods and environmental hazard assessment for engineered nanoparticles. *Ecotoxicology* 17, 421–437.
- Della Torre, C., Bergami, E., Salvati, A., Faleri, C., Cirino, P., Dawson, K.A., Corsi, I., 2014. Accumulation and embryotoxicity of polystyrene nanoparticles at early stage of development of sea urchin embryos *Paracentrotus lividus*. *Environ. Sci. Technol.* 48, 12302–12311.
- Fleischer, C.C., Payne, C.K., 2014. Nanoparticle-cell interactions: molecular structure of the protein corona and cellular outcomes. *Acc. Chem. Res.* 47, 2651–2659.
- Hidalgo-Ruz, V., Gutow, L., Thompson, R.C., Thiel, M., 2012. Microplastics in the marine environment: a review of the methods used for identification and quantification. *Environ. Sci. Technol.* 46, 3060–3075.
- Jovanovic, B., Palic, D., 2012. Immunotoxicology of non-functionalized engineered nanoparticles in aquatic organisms with special emphasis on fish-review of current knowledge, gap identification, and call for further research. *Aquat. Toxicol.* 15, 118–119.
- Liu, Y.X., Li, W., Lao, F., Liu, Y., Wang, L.M., Bai, R., 2011. Intracellular dynamics of cationic and anionic polystyrene nanoparticles without direct interaction with mitotic spindle and chromosomes. *Biomaterials* 32, 8291–8303.
- Lundqvist, M., Stigler, J., Elia, G., Lynch, I., Cedervall, T., Dawson, K.A., 2008. Nanoparticle size and surface properties determine the protein corona with possible implications for biological impacts. *Proc. Natl. Acad. Sci. U. S. A.* 105, 14265–14270.
- Lunov, O., Syrovets, T., Loos, C., Nienhaus, U., Mailänder, V., Landfester, K., Rouis, M., Simmet, T., 2011. Amino-functionalized polystyrene nanoparticles activate the NLRP3 inflammasome in human macrophages. *ACS Nano* 5, 9648–9657.
- Matranga, V., Corsi, I., 2012. Toxic effects of engineered nanoparticles in the marine environment: model organisms and molecular approaches. *Mar. Environ. Res.* 76, 32–40.
- Moore, M.N., 2006. Do nanoparticles present ecotoxicological risks for the health of the aquatic environment? *Environ. Int.* 32, 967–976.
- Nel, A.E., Madler, L., Velegol, D., Xia, T., Hoek, E.M.V., Somasundaran, P., 2009. Understanding biophysicochemical interactions at the nano-bio interface. *Nat. Mater.* 8, 543–557.
- Oliveri, C., Peric, L., Sforzini, S., Banni, M., Viarengo, A., Cavaletto, M., Marsano, F., 2014. Biochemical and proteomic characterisation of haemolymph serum reveals the origin of the alkali-labile phosphate (ALP) in mussel (*Mytilus galloprovincialis*). *Comp. Biochem. Physiol. Part D. Genomics Proteomics* 11, 29–36.
- PlasticsEurope, 2013. *Plastics – the Facts 2013: an Analysis of European Latest Plastics Production, Demand and Waste Data*. <http://www.plasticseurope.org/Document/plastics-the-facts-2013.aspx>.
- Stern, S.T., Adiseshiaiah, P.P., Crist, R.M., 2012. Autophagy and lysosomal dysfunction as emerging mechanisms of nanomaterial toxicity. *Part. Fibre Toxicol.* 9, 20.
- Sun, T.Y., Gottschalk, F., Hungerbühler, K., Nowack, B., 2014. Comprehensive probabilistic modelling of environmental emissions of engineered nanomaterials. *Environ. Pollut.* 185, 69–76.
- Van Cauwenbergh, L., Janssen, C.R., 2014. Microplastics in bivalves cultured for human consumption. *Environ. Pollut.* 193, 65–70.
- Wang, F., Bexiga, M.G., Anguissola, S., Boya, P., Simpson, J.C., Salvati, A., Dawson, K.A., 2013. Time resolved study of cell death mechanisms induced by amine-modified polystyrene nanoparticles. *Nanoscale* 5, 10868–10876.
- Ward, J.E., Kach, D., 2009. Marine aggregates facilitate ingestion of nanoparticles by suspension-feeding bivalves. *Mar. Environ. Res.* 68, 137–142.
- Wegner, A., Besseling, E., Foekema, E.M., Kamermans, P., Koelmans, A., 2012. Effects of nanopolystyrene on the feeding behavior of the blue mussel (*Mytilus edulis* L.). *Environ. Toxicol. Chem.* 31, 2490–2497.
- Wright, S.L., Thompson, R.C., Galloway, T.S., 2013. The physical impacts of microplastics on marine organisms: a review. *Environ. Pollut.* 178, 483–492.